Search for lepton flavor and lepton number violating τ decays into a lepton and two charged mesons

Belle Collaboration

Y. Miyazaki [x,*], H. Aihara [ar], K. Arinstein [a,ag], V. Aulchenko [a,ag], T. Aushev [s,c], A.M. Bakich [an], V. Balagura [m], E. Barberio [w], A. Bay [s], K. Belous [k], V. Bhardwaj [ai], M. Bischofberger [y], A. Bondar [a,ag], M. Bračko [u,n], T.E. Browder [g], P. Chang [ab], A. Chen [z], B.G. Cheon [f], I.-S. Cho [av], Y. Choi [am], J. Dalseno [v,ao], M. Dash [au], W. Dungel [l], S. Eidelman [a,ag], D. Epifanov [a,ag], M. Feindt [p], N. Gabyshev [a,ag], A. Garmash [a,ag], P. Goldenzweig [c], H. Ha [q], J. Haba [h], K. Hara [x], Y. Hasegawa [al], K. Hayasaka [x], H. Hayashii [y], Y. Horii [aq], Y. Hoshi [ap], W.-S. Hou [ab], H.J. Hyun [r], T. Iijima [x], K. Inami [x], R. Itoh [h], M. Iwasaki [ar], Y. Iwasaki [h], T. Julius [w], D.H. Kah [r], J.H. Kang [av], H. Kawai [b], T. Kawasaki [ae], H.O. Kim [r], J.H. Kim [am], S.K. Kim [ak], Y.I. Kim [r], Y.J. Kim [e], B.R. Ko [q], S. Korpar [u,n], P. Križan [t,n], P. Krokovny [h], R. Kumar [ai], T. Kumita [as], A. Kuzmin [a,ag], Y.-J. Kwon [av], S.-H. Kyeong [av], S.-H. Lee [au], T. Lesiak [ac,d], J. Li [g], C. Liu [aj], D. Liventsev [m], R. Louvot [s], A. Matyja [ac], S. McOnie [an], K. Miyabayashi [y], H. Miyata [ae], T. Nagamine [aq], Y. Nagasaka [i], E. Nakano [ah], M. Nakao [h], S. Nishida [h], K. Nishimura [g], O. Nitoh [at], T. Ohshima [x], S. Okuno [o], S.L. Olsen [g], P. Pakhlov [m], G. Pakhlova [m], H. Palka [ac], C.W. Park [am], H. Park [r], H.K. Park [r], R. Pestotnik [n], L.E. Piilonen [au], A. Poluektov [a,ag], Y. Sakai [h], O. Schneider [s], C. Schwanda [l], K. Senyo [x], M. Shapkin [k], V. Shebalin [a,ag], J.-G. Shiu [ab], B. Shwartz [a,ag], A. Sokolov [k], E. Solovieva [m], S. Stanič [af], M. Starič [n], T. Sumiyoshi [as], G.N. Taylor [w], Y. Teramoto [ah], I. Tikhomirov [m], S. Uehara [h], Y. Unno [f], S. Uno [h], P. Urquijo [w], Y. Usov [a,ag], G. Varner [g], A. Vinokurova [a,ag], C.H. Wang [aa], P. Wang [j], Y. Watanabe [o], R. Wedd [w], E. Won [q], B.D. Yabsley [an], Y. Yamashita [ad], Y. Yusa [au], Z.P. Zhang [aj], V. Zhilich [a,ag], V. Zhulanov [a,ag], T. Zivko [n], A. Zupanc [n], O. Zyukova [a,ag]

[a] *Budker Institute of Nuclear Physics, Novosibirsk, Russian Federation*
[b] *Chiba University, Chiba, Japan*
[c] *University of Cincinnati, Cincinnati, OH, USA*
[d] *T. Kościuszko Cracow University of Technology, Krakow, Poland*
[e] *The Graduate University for Advanced Studies, Hayama, Japan*
[f] *Hanyang University, Seoul, South Korea*
[g] *University of Hawaii, Honolulu, HI, USA*
[h] *High Energy Accelerator Research Organization (KEK), Tsukuba, Japan*
[i] *Hiroshima Institute of Technology, Hiroshima, Japan*
[j] *Institute of High Energy Physics, Chinese Academy of Sciences, Beijing, PR China*
[k] *Institute for High Energy Physics, Protvino, Russian Federation*
[l] *Institute of High Energy Physics, Vienna, Austria*
[m] *Institute for Theoretical and Experimental Physics, Moscow, Russian Federation*
[n] *J. Stefan Institute, Ljubljana, Slovenia*
[o] *Kanagawa University, Yokohama, Japan*
[p] *Institut für Experimentelle Kernphysik, Universität Karlsruhe, Karlsruhe, Germany*
[q] *Korea University, Seoul, South Korea*
[r] *Kyungpook National University, Taegu, South Korea*
[s] *École Polytechnique Fédérale de Lausanne, EPFL, Lausanne, Switzerland*
[t] *Faculty of Mathematics and Physics, University of Ljubljana, Ljubljana, Slovenia*
[u] *University of Maribor, Maribor, Slovenia*
[v] *Max-Planck-Institut für Physik, München, Germany*
[w] *University of Melbourne, Victoria, Australia*
[x] *Nagoya University, Nagoya, Japan*

* Corresponding author.
E-mail address: miya@hepl.phys.nagoya-u.ac.jp (Y. Miyazaki).

[y] *Nara Women's University, Nara, Japan*
[z] *National Central University, Chung-li, Taiwan*
[aa] *National United University, Miao Li, Taiwan*
[ab] *Department of Physics, National Taiwan University, Taipei, Taiwan*
[ac] *H. Niewodniczanski Institute of Nuclear Physics, Krakow, Poland*
[ad] *Nippon Dental University, Niigata, Japan*
[ae] *Niigata University, Niigata, Japan*
[af] *University of Nova Gorica, Nova Gorica, Slovenia*
[ag] *Novosibirsk State University, Novosibirsk, Russian Federation*
[ah] *Osaka City University, Osaka, Japan*
[ai] *Panjab University, Chandigarh, India*
[aj] *University of Science and Technology of China, Hefei, PR China*
[ak] *Seoul National University, Seoul, South Korea*
[al] *Shinshu University, Nagano, Japan*
[am] *Sungkyunkwan University, Suwon, South Korea*
[an] *School of Physics, University of Sydney, NSW 2006, Australia*
[ao] *Excellence Cluster Universe, Technische Universität München, Garching, Germany*
[ap] *Tohoku Gakuin University, Tagajo, Japan*
[aq] *Tohoku University, Sendai, Japan*
[ar] *Department of Physics, University of Tokyo, Tokyo, Japan*
[as] *Tokyo Metropolitan University, Tokyo, Japan*
[at] *Tokyo University of Agriculture and Technology, Tokyo, Japan*
[au] *IPNAS, Virginia Polytechnic Institute and State University, Blacksburg, VA, USA*
[av] *Yonsei University, Seoul, South Korea*

ARTICLE INFO

ABSTRACT

We search for lepton flavor and lepton number violating τ decays into a lepton ($\ell =$ electron or muon) and two charged mesons ($h, h' = \pi^{\pm}$ or $K^{\pm}$), $\tau^- \to \ell^- h^+ h'^-$ and $\tau^- \to \ell^+ h^- h'^-$, using 671 fb^{-1} of data collected with the Belle detector at the KEKB asymmetric-energy $e^+ e^-$ collider. We obtain 90% C.L. upper limits on the branching fractions in the range $(4.4–8.8) \times 10^{-8}$ for $\tau \to ehh'$, and $(3.3–16) \times 10^{-8}$ for $\tau \to \mu hh'$ processes. These results improve upon previously published upper limits by factors between 1.6 to 8.8.

1. Introduction

Lepton flavor violation (LFV) in charged lepton decays is forbidden or highly suppressed even if neutrino mixing is included. However, LFV appears in various extensions of the Standard Model (SM), such as supersymmetry, leptoquark and many other models [1–8]. Some of these models predict branching fractions which, for certain combinations of model parameters, can be as high as 10^{-7}; these rates are already accessible in high-statistics B-factory experiments. Here, we search for τ decays[1] into one lepton ($\ell =$ electron or muon) and two charged mesons ($h, h' = \pi^{\pm}$ or $K^{\pm}$) including lepton flavor and lepton number violation ($\tau^- \to \ell^- h^- h'^+$ and $\tau^- \to \ell^+ h^- h'^-$),[2] with a data sample of 671 fb^{-1} collected at the $\Upsilon(4S)$ resonance and 60 MeV below with the Belle detector at the KEKB asymmetric-energy $e^+ e^-$ collider [9]. Previously, we reported 90% confidence level (C.L.) upper limits on these LFV branching fractions using 158 fb^{-1} of data; the results were in the range $(1.6–8.0) \times 10^{-7}$ [10]. The BaBar Collaboration has also obtained 90% C.L. upper limits in the range $(0.7–4.8) \times 10^{-7}$ using 221 fb^{-1} of data [11].

The Belle detector is a large-solid-angle magnetic spectrometer that consists of a silicon vertex detector (SVD), a 50-layer central drift chamber (CDC), an array of aerogel threshold Cherenkov counters (ACC), a barrel-like arrangement of time-of-flight scintillation counters (TOF), and an electromagnetic calorimeter comprised of CsI(Tl) crystals (ECL), all located inside a superconducting solenoid coil that provides a 1.5 T magnetic field. An iron flux-return located outside the coil is instrumented to detect K_L^0 mesons and to identify muons (KLM). The detector is described in detail elsewhere [12].

Particle identification is very important for this measurement. We use hadron identification likelihood variables based on the ratio of the energy deposited in the ECL to the momentum measured in the SVD and CDC, the shower shape in the ECL, the particle range in the KLM, the hit information from the ACC, the dE/dx information in the CDC, and the particle time-of-flight from the TOF. To distinguish hadron species, we use likelihood ratios, $\mathcal{P}(i/j) = \mathcal{L}_i/(\mathcal{L}_i + \mathcal{L}_j)$, where $\mathcal{L}_i$ ($\mathcal{L}_j$) is the likelihood for the detector response to a track with flavor hypothesis i (j). For lepton identification, we form likelihood ratios $\mathcal{P}(e)$ [13] and $\mathcal{P}(\mu)$ [14] based on the electron and muon probabilities, respectively, which are determined by the responses of the appropriate subdetectors.

In order to estimate the signal efficiency and optimize the event selection, we use Monte Carlo (MC) simulated event samples. The signal and background events from generic $\tau^+ \tau^-$ decays are generated by KKMC/TAUOLA [15]. For the signal MC sample, we generate $\tau^+ \tau^-$ pairs, where one τ decays into a lepton and two charged mesons, using a three-body phase space model, and the other τ decays generically. Other backgrounds, including $B\bar{B}$ and continuum $e^+ e^- \to q\bar{q}$ ($q = u, d, s, c$) events, Bhabha events,

---

[1] Throughout this Letter, charge-conjugate modes are implied unless stated otherwise.

[2] The notation "$\tau \to \ell hh'$" indicates both $\tau^- \to \ell^- h^+ h'^-$ and $\tau^- \to \ell^+ h^- h'^-$ modes.

and two-photon processes are generated by EvtGen [16], BHLUMI [17], and AAFH [18], respectively. The event selection is optimized mode-by-mode since the backgrounds are mode dependent. All kinematic variables are calculated in the laboratory frame unless otherwise specified. In particular, variables calculated in the e^+e^- center-of-mass (CM) system are indicated by the superscript "CM".

2. Event selection

Since the majority of τ decays produce one-prong final states [19], we search for $\tau^+\tau^-$ events in which one τ (the signal τ) decays into a lepton and two charged mesons ($\pi^\pm$ or $K^\pm$) and the other τ (the tag τ) decays into one charged track with any number of additional photons and neutrinos. Candidate τ-pair events are required to have four tracks with zero net charge.

We start by reconstructing four charged tracks and any number of photons within the fiducial volume defined by $-0.866 < \cos\theta < 0.956$, where θ is the polar angle relative to the direction opposite to that of the incident e^+ beam in the laboratory frame. The transverse momentum (p_t) of each charged track and the energy of each photon (E_γ) are required to satisfy $p_t > 0.1$ GeV/c and $E_\gamma > 0.1$ GeV, respectively. For each charged track, the distance of the closest point with respect to the interaction point is required to be less than 0.5 cm in the transverse direction and less than 3.0 cm in the longitudinal direction.

Using the plane perpendicular to the CM thrust axis [20], which is calculated from the observed tracks and photon candidates, we separate the particles in an event into two hemispheres. These are referred to as the signal and tag sides. The tag side contains one charged track while the signal side contains three charged tracks. We require one charged track on the signal side to be identified as a lepton. The lepton identification criteria are $\mathcal{P}(\ell) > 0.95$ and the momentum thresholds are listed in Table 1. The electron (muon) identification efficiency is 91% (85%) while the probability to misidentify a pion as an electron (a muon) is below 0.5% (2%). In order to take into account the emission of bremsstrahlung photons from the electron, the momentum of each electron track is reconstructed by adding the momentum of every photon within 0.05 rad along the track. To reduce generic $\tau^+\tau^-$ and $q\bar{q}$ background events, we veto events that have a photon on the signal side.

To ensure that the missing particles are neutrinos rather than photons or charged particles that pass outside the detector acceptance, we impose requirements on the missing momentum $\vec{p}_{\text{miss}}$, which is calculated by subtracting the vector sum of the momenta of all tracks and photons from the sum of the e^+ and e^- beam momenta. We require that the magnitude of $\vec{p}_{\text{miss}}$ be greater than 1.0 GeV/c, and that its direction point into the fiducial volume of the detector. Furthermore, we reject the event if the direction of the missing momentum traverses the gap between the barrel and endcap of the ECL. Since neutrinos are emitted only on the tag side, the direction of $\vec{p}_{\text{miss}}$ should lie within the tag side of the event. The cosine of the opening angle between $\vec{p}_{\text{miss}}$ and the charged track on the tag side in the CM system, $\cos\theta_{\text{tag-miss}}^{\text{CM}}$, should be in the range $0.4 < \cos\theta_{\text{tag-miss}}^{\text{CM}} < 0.98$.

The remaining two tracks on the signal side are identified as $K^\pm$ ($\pi^\pm$) if they satisfy the condition $\mathcal{P}(K/\pi) > 0.8$ (< 0.4). If either track has a value in the intermediate range, $0.4 < \mathcal{P}(K/\pi) < 0.8$, the event is rejected. The kaon (pion) identification efficiency is 80% (88%) while the probability to misidentify a pion (kaon) as a kaon (a pion) is below 10% (12%). In order to reduce background from mesons reconstructed from photon conversions (i.e. $\gamma \to e^+e^-$), we require that two charged meson candidates have $\mathcal{P}(e) < 0.1$. Furthermore, we require $\mathcal{P}(\mu) < 0.1$ to suppress the two-photon background process $e^+e^- \to e^+e^-\mu^+\mu^-$.

To reject $q\bar{q}$ background, we require the magnitude of the thrust (T) to be in the ranges given in Table 1 (see Figs. 1(a) and 2(a)). We also require 5.5 GeV $< E_{\text{vis}}^{\text{CM}} <$ 10.0 GeV, where $E_{\text{vis}}^{\text{CM}}$ is the total visible energy in the CM system, defined as the sum of the energies of the lepton, two charged mesons, the charged track on the tag side (with a pion mass hypothesis) and all photon candidates (see Fig. 1(b)). The invariant mass reconstructed from the charged track and any photons on the tag side m_{tag}, is required to be less than 1.00 GeV/c^2 (see Fig. 2(b)). In order to reduce $q\bar{q}$ background, a kaon veto $\mathcal{P}(K/\pi) < 0.8$ is applied to the lepton and tracks on the tag side for the $\mu\pi K$ and $\mu K K$ modes.

We remove events if K_S^0 candidates are reconstructed from two oppositely-charged tracks on the signal side with an invariant mass 0.470 GeV/$c^2 < M_{\pi^+\pi^-} < 0.525$ GeV/c^2, assuming the pion mass for both tracks, and the $\pi^+\pi^-$ vertex is displaced from the interaction point (IP) in the direction of the pion pair momentum [21]. Events including a K_L^0 meson also constitute background since the undetected K_L^0 results in fake missing momentum. Therefore, we veto events with K_L^0 candidates, which are selected from hit clus-

Table 1
Selection criteria for lepton momentum (p_ℓ) and magnitude of thrust (T).

Mode	p_ℓ (GeV/c)	T
$\tau \to \mu\pi\pi$	$p_\mu > 1.4$	$0.90 < T < 0.97$
$\tau \to \mu K\pi$	$p_\mu > 1.1$	$0.92 < T < 0.98$
$\tau \to \mu K K$	$p_\mu > 0.8$	$0.92 < T < 0.98$
$\tau \to e\pi\pi$	$p_e > 0.6$	$0.90 < T < 0.97$
$\tau \to e K\pi$	$p_e > 0.4$	$0.90 < T < 0.97$
$\tau \to e K K$	$p_e > 0.4$	$0.90 < T < 0.98$

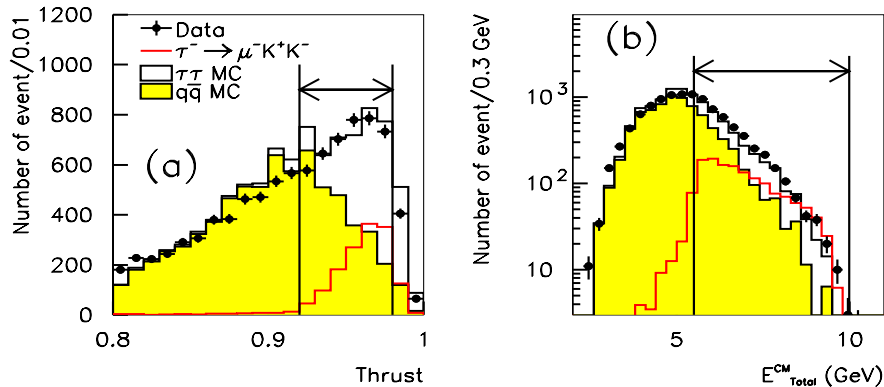**Fig. 1.** Distribution of (a) the magnitude of thrust and (b) the total visible energy in the CM system. While the signal MC ($\tau^- \to \mu^- K^+K^-$) distribution is normalized arbitrarily, the data and background MC are normalized to the same luminosity. The selected regions are indicated by the arrows.
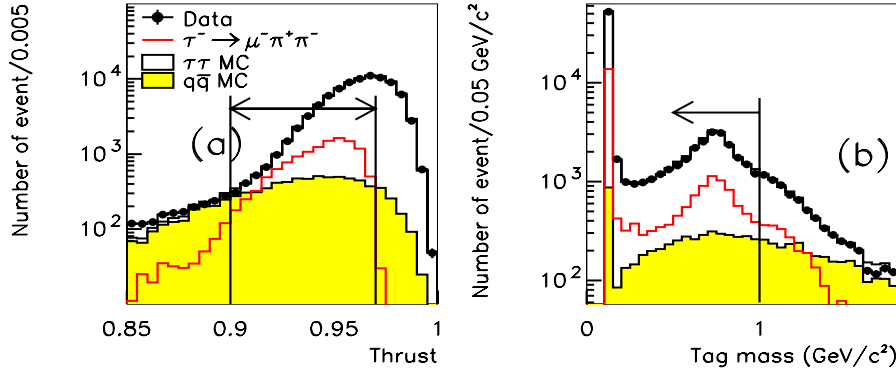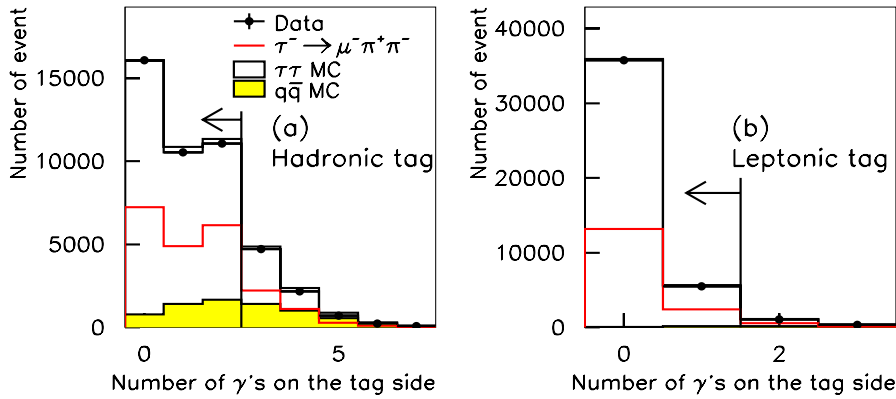
Fig. 2. Distribution of (a) the magnitude of thrust and (b) invariant mass using particles on the tag side. While the signal MC ($\tau^- \to \mu^- \pi^+ \pi^-$) distribution is normalized arbitrarily, the data and background MC are normalized to the same luminosity. The selected regions are indicated by the arrows.

Fig. 3. Distributions of the number of photons on the tag side for (a) hadronic and (b) leptonic tags. While the signal MC ($\tau^- \to \mu^- \pi^+ \pi^-$) distribution is normalized arbitrarily, the data and background MC are normalized to the same luminosity. The selected regions are indicated by the arrows.

ters in the KLM that are not associated with either an ECL cluster or with a charged track [22], for the $\mu hh'$ modes.

To suppress the $B\bar{B}$ and $q\bar{q}$ background, we require that the number of photons on the tag side n_γ^{TAG} be $n_\gamma^{\text{TAG}} \leqslant 2$ and $n_\gamma^{\text{TAG}} \leqslant 1$ for hadronic and leptonic tag decays, respectively (see Fig. 3). For all kinematic distributions shown in Figs. 1, 2 and 3, reasonable agreement between the data and background MC is observed.

To reduce two-photon background, we apply an electron veto $\mathcal{P}(e) < 0.1$ to the track on the tag side for the $e\pi\pi$ and $e\pi K$ modes. Furthermore, we require that the momentum of the electron and track on the tag side in the CM system be less than 4.5 GeV/c to reduce Bhabha background in the $e\pi\pi$ modes.

Finally, to suppress backgrounds from generic $\tau^+\tau^-$ and $q\bar{q}$ events, we apply a selection based on the magnitude of the missing momentum p_{miss} and the missing mass squared m_{miss}^2. We apply different selection criteria depending on the lepton identification of the charged track on the tag side; two neutrinos are emitted if the track is an electron or muon (leptonic tag) while only one is emitted if the track is a hadron (hadronic tag). For the ehh', $\mu\pi\pi$ and μKK modes, we require the following relation between p_{miss} and m_{miss}^2: $p_{\text{miss}} > -7.0 \times m_{\text{miss}}^2 - 1.0$ and $p_{\text{miss}} > 7.0 \times m_{\text{miss}}^2 - 1.0$ for the hadronic tag and $p_{\text{miss}} > -8.0 \times m_{\text{miss}}^2 + 0.2$ and $p_{\text{miss}} > 1.8 \times m_{\text{miss}}^2 - 0.4$ for the leptonic tag, where p_{miss} is in GeV/c and m_{miss} is in GeV/c^2 (see Fig. 4). For the $\mu\pi K$ modes, we require the following relation between p_{miss} and m_{miss}^2: $p_{\text{miss}} > -8.0 \times m_{\text{miss}}^2 - 0.5$ and $p_{\text{miss}} > 8.0 \times m_{\text{miss}}^2 - 0.5$ for the hadronic tag and $p_{\text{miss}} > -9.0 \times m_{\text{miss}}^2 + 0.4$ and $p_{\text{miss}} > 1.8 \times m_{\text{miss}}^2 - 0.4$ for the leptonic tag.

Table 2

Summary of $M_{\ell hh'}$ and ΔE resolutions ($\sigma_{M_{\ell hh'}}^{\text{high/low}}$ (MeV/c^2) and $\sigma_{\Delta E}^{\text{high/low}}$ (MeV)). Here σ^{high} (σ^{low}) means the standard deviation on the higher (lower) side of the peak.

Mode	$\sigma_{M_{\ell hh'}}^{\text{high}}$	$\sigma_{M_{\ell hh'}}^{\text{low}}$	$\sigma_{\Delta E}^{\text{high}}$	$\sigma_{\Delta E}^{\text{low}}$
$\tau^- \to \mu^- \pi^+ \pi^-$	4.8	5.5	13.7	18.0
$\tau^- \to \mu^+ \pi^- \pi^-$	5.3	5.4	14.1	18.8
$\tau^- \to e^- \pi^+ \pi^-$	5.3	5.9	14.7	21.2
$\tau^- \to e^+ \pi^- \pi^-$	5.6	5.9	14.2	21.3
$\tau^- \to \mu^- K^+ K^-$	3.6	4.0	11.4	18.0
$\tau^- \to \mu^+ K^- K^-$	3.4	3.6	11.4	18.8
$\tau^- \to e^- K^+ K^-$	4.0	4.3	13.7	20.5
$\tau^- \to e^+ K^- K^-$	3.5	4.5	13.9	21.3
$\tau^- \to \mu^- \pi^+ K^-$	4.5	5.0	13.6	18.6
$\tau^- \to e^- \pi^+ K^-$	4.7	5.4	13.6	21.7
$\tau^- \to \mu^- K^+ \pi^-$	4.6	5.1	14.3	18.3
$\tau^- \to e^- K^+ \pi^-$	4.6	5.5	13.5	21.6
$\tau^- \to \mu^+ K^- \pi^-$	4.5	5.0	12.4	18.6
$\tau^- \to e^+ K^- \pi^-$	4.9	5.3	13.0	20.8

3. Signal and background estimation

The signal candidates are examined in the two-dimensional plot of the $\ell hh'$ invariant mass ($M_{\ell hh'}$) versus the difference of their energy from the beam energy in the CM system (ΔE). A signal event should have $M_{\ell hh'}$ close to the τ-lepton mass (m_τ) and ΔE close to zero. For all modes, the $M_{\ell hh'}$ and ΔE resolutions are parameterized from fits to the signal MC distributions, with an asymmetric Gaussian function that takes into account initial-state radiation. The resolutions in $M_{\ell hh'}$ and ΔE are listed in Table 2.
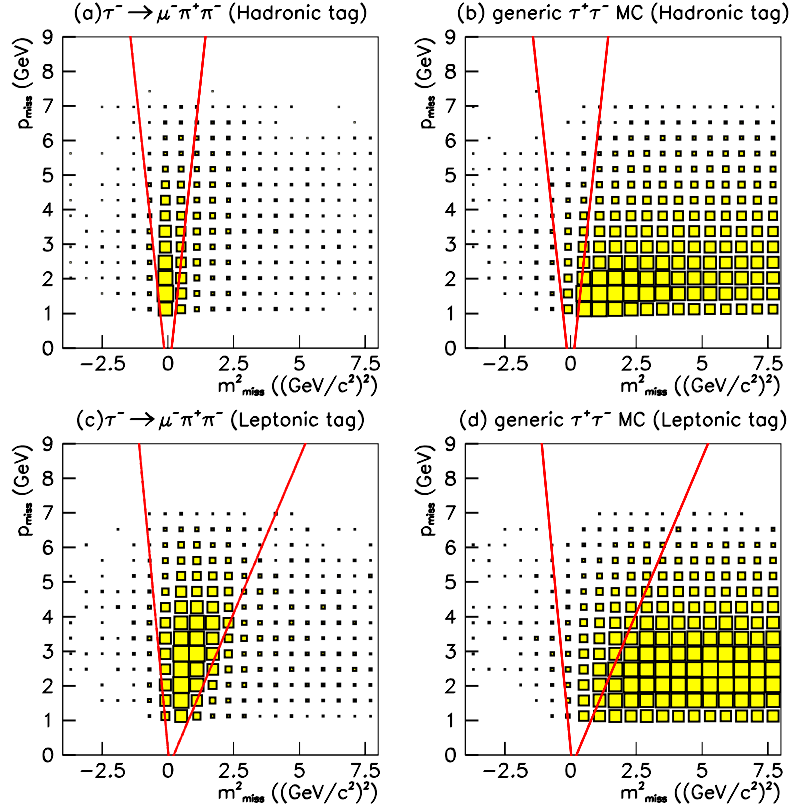
Fig. 4. Scatter-plots of p_{miss} vs. m^2_{miss}: (a) and (b) show the signal MC ($\tau^- \to \mu^- \pi^+ \pi^-$) and generic $\tau^+\tau^-$ MC distributions, respectively, for the hadronic tags while (c) and (d) are the same distributions for the leptonic tags. The selected regions are indicated by lines.
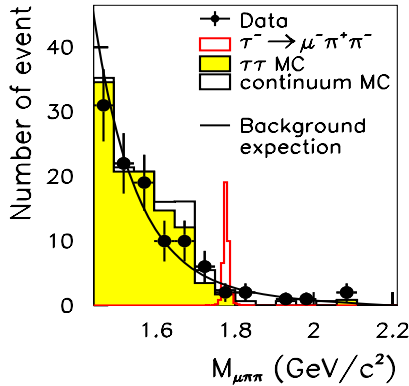

Fig. 5. Mass distribution of $\mu^- \pi^+ \pi^-$ within the $\pm 5\sigma_{\Delta E}$ region after event selection. While the signal MC ($\tau^- \to \mu^- \pi^+ \pi^-$) distribution is normalized arbitrarily, the data and background MC are normalized to the same luminosity. The expected background is shown as the solid histogram.

Table 3
The signal efficiency (ε), the number of expected background events (N_{BG}) estimated from the sideband data, the total systematic uncertainty (σ_{syst}), the number of observed events in the signal region (N_{obs}), 90% C.L. upper limit on the number of signal events including systematic uncertainties (s_{90}) and 90% C.L. upper limit on the branching fraction for each individual mode.

Mode	ε (%)	N_{BG}	σ_{syst} (%)	N_{obs}	s_{90}	$\mathcal{B}$ (10^{-8})
$\tau^- \to \mu^- \pi^+ \pi^-$	3.69	1.12 ± 0.38	5.9	0	1.53	3.3
$\tau^- \to \mu^+ \pi^- \pi^-$	3.84	0.73 ± 0.25	5.9	0	1.77	3.7
$\tau^- \to e^- \pi^+ \pi^-$	3.99	0.34 ± 0.15	6.0	0	2.15	4.4
$\tau^- \to e^+ \pi^- \pi^-$	3.91	0.10 ± 0.07	6.0	1	4.21	8.8
$\tau^- \to \mu^- K^+ K^-$	2.40	0.52 ± 0.23	6.7	0	1.92	6.8
$\tau^- \to \mu^+ K^- K^-$	2.07	$0.00^{+0.06}_{-0.00}$	6.8	0	2.46	9.6
$\tau^- \to e^- K^+ K^-$	3.50	0.11 ± 0.08	6.5	0	2.35	5.4
$\tau^- \to e^+ K^- K^-$	3.28	0.05 ± 0.05	6.6	0	2.43	6.0
$\tau^- \to \mu^- \pi^+ K^-$	2.63	0.67 ± 0.14	6.3	2	5.05	16
$\tau^- \to e^- \pi^+ K^-$	3.02	0.33 ± 0.19	6.4	0	2.12	5.8
$\tau^- \to \mu^- K^+ \pi^-$	2.60	1.04 ± 0.32	6.3	1	3.34	10
$\tau^- \to e^- K^+ \pi^-$	2.98	0.57 ± 0.19	6.4	0	1.90	5.2
$\tau^- \to \mu^+ K^- \pi^-$	2.61	1.37 ± 0.21	6.3	1	3.16	9.4
$\tau^- \to e^+ K^- \pi^-$	2.83	0.10 ± 0.07	6.4	0	2.40	6.7

To evaluate the branching fractions, we use elliptical signal regions that contain 90% of the signal MC events satisfying all selection criteria. These regions are determined by scanning ellipse parameters to minimize the ellipse area and obtain the highest sensitivity. The obtained ellipse parameters are correlated to those in Table 2, but there are no straightforward relations between them. We blind the data in the signal region until all selection criteria are finalized so as not to bias our choice of selection criteria.

For the ehh' modes the dominant background is from two-photon processes; the fraction of $q\bar{q}$ and generic $\tau^+\tau^-$ events is small due to the low electron fake rate. For the $\mu\pi\pi$ mode the dominant background is from $q\bar{q}$ processes and a smaller back-

ground is from generic $\tau^+\tau^-$ events in the $\Delta E < 0$ GeV and $M_{\mu\pi\pi} < m_\tau$ region, which are combinations of a fake muon and two pions. For the $\mu\pi K$ mode, the dominant background is from generic $\tau^+\tau^-$ events that are combinations of a fake muon, a fake kaon and a true pion. If a pion is misidentified as a kaon, the reconstructed mass from generic $\tau^+\tau^-$ background can be greater than the τ-lepton mass because of the larger kaon mass. For the μKK mode, the dominant background originates from $q\bar{q}$ events and $\tau^+\tau^-$ events.

The number of background events in the signal region is estimated from the data remaining after event selection in the side-
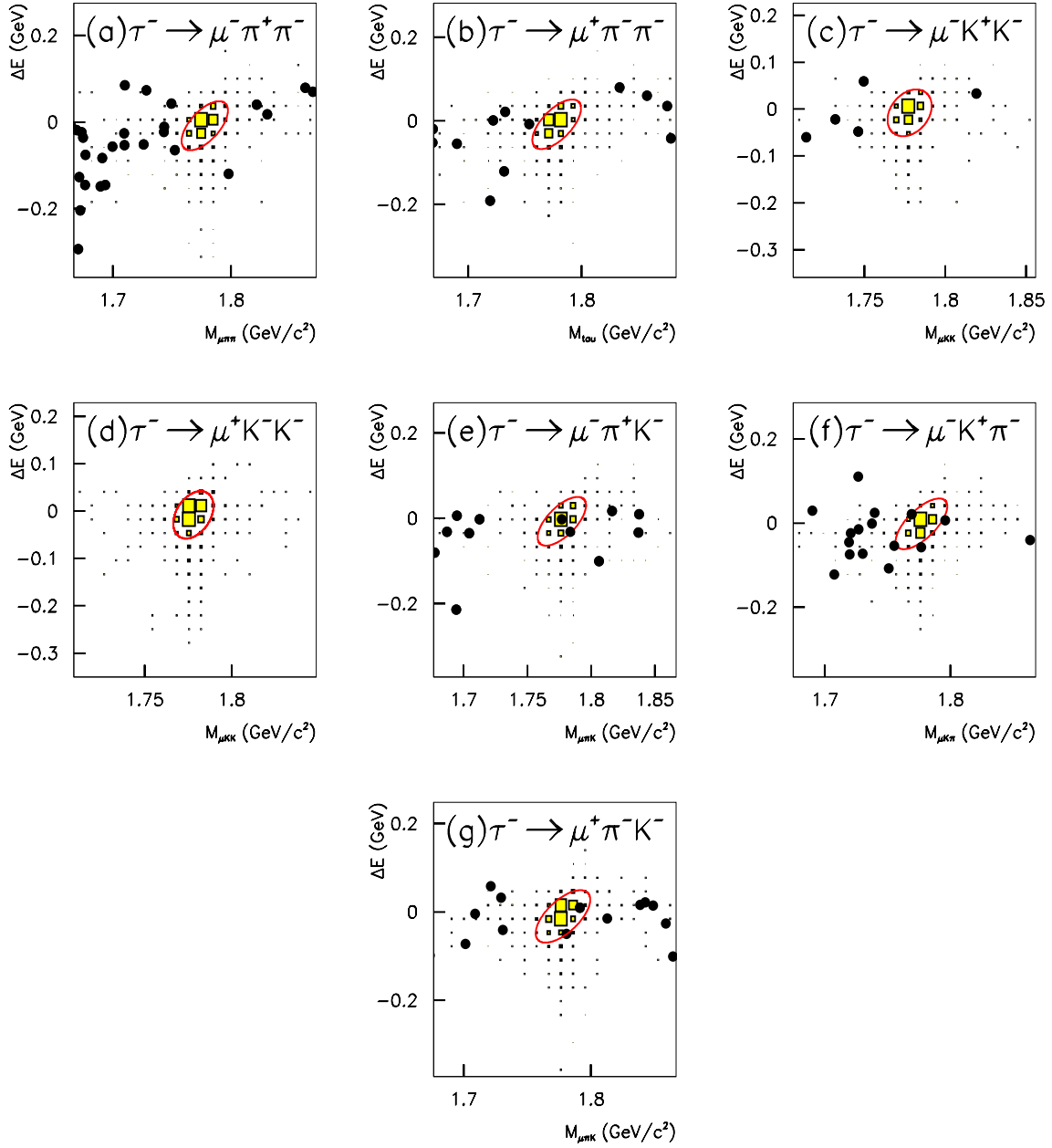
Fig. 6. Scatter-plots in the $M_{\ell h h'} - \Delta E$ plane within the $\pm 20\sigma$ area for the (a) $\tau^- \to \mu^- \pi^+ \pi^-$, (b) $\tau^- \to \mu^+ \pi^- \pi^-$, (c) $\tau^- \to \mu^- K^+ K^-$, (d) $\tau^- \to \mu^+ K^- K^-$, (e) $\tau^- \to \mu^- \pi^+ K^-$, (f) $\tau^- \to \mu^- K^+ \pi^-$, and (g) $\tau^- \to \mu^+ \pi^- K^-$ modes. The data are indicated by the solid circles. The filled boxes show the MC signal distribution with arbitrary normalization. The elliptical signal regions shown by the solid curves are used for evaluating the signal yield.

band region. For the ehh' and μKK modes, since the number of remaining data events is small, the number of background events in the signal region is estimated by interpolating the number of observed events in the sideband region defined as the range $\pm 20\sigma_{M_{\ell h h'}}$ and $\pm 5\sigma_{\Delta E}$ excluding the signal region, assuming that the background distribution is uniform in the sideband region. For the $\mu \pi \pi$ and $\mu \pi K$ modes, we estimate the number of background events in the signal region by fitting to observed data in the sideband region using a probability density function (PDF) that describes the shapes of the background distributions along the $M_{\mu \pi \pi}$ axis within $\pm 5\sigma_{\Delta E}$. For the $\mu \pi \pi$ mode, the PDFs of generic $\tau \tau$ and $q \bar{q}$ events are determined using MC samples, assuming exponential and first-order polynomial distributions, respectively (see Fig. 5). For the $\mu \pi K$ modes, we parameterize the PDF by a 3rd-order polynomial function that is fitted to the data remaining in

the sideband region. The signal efficiency and the number of expected background events in the signal region for each mode are summarized in Table 3. (See Figs. 6 and 7.)

The dominant systematic uncertainties for this analysis come from tracking efficiencies and particle identification. The uncertainty due to the charged track finding is estimated to be 1.0% per charged track; the total uncertainty due to the charged track finding is 4.0%. The uncertainties due to lepton identification are 2.2% and 1.9% for electron and muon, respectively. The uncertainty due to pion and kaon identification is 1.3% and 1.8% per pion and kaon, respectively. The uncertainty due to the e-veto on the tag side applied for the $\tau \to e \pi \pi$ and $\tau \to e \pi K$ modes is estimated as the uncertainty in the electron identification times the branching fraction of $\tau^- \to e^- \bar{\nu}_e \nu_\tau$ (0.4%). Therefore, total uncertainties from particle identification are (3.2–4.2)%. The other uncertainties due
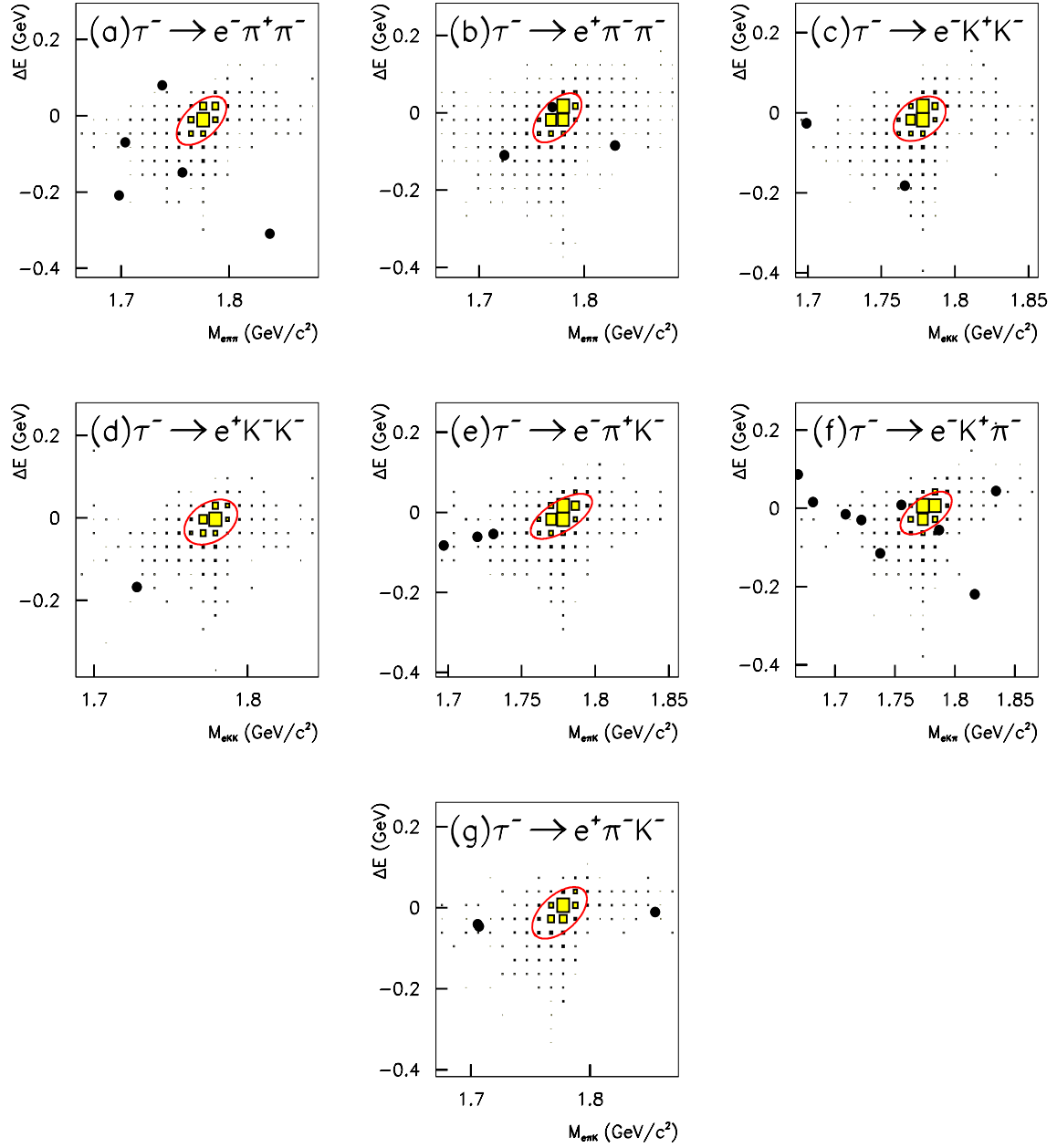
Fig. 7. Scatter-plots in the $M_{\ell hh'} - \Delta E$ plane within the $\pm 20\sigma$ area for the (a) $\tau^- \to e^- \pi^+ \pi^-$, (b) $\tau^- \to e^+ \pi^- \pi^-$, (c) $\tau^- \to e^- K^+ K^-$, (d) $\tau^- \to e^+ K^- K^-$, (e) $\tau^- \to e^- \pi^+ K^-$, (f) $\tau^- \to e^- K^+ \pi^-$, and (g) $\tau^- \to e^+ \pi^- K^-$ modes. The data are indicated by the solid circles. The filled boxes show the MC signal distribution with arbitrary normalization. The elliptical signal regions shown by the solid curves are used for evaluating the signal yield.

to MC statistics and luminosity are estimated to be (2.5–3.4)% and 1.4%, respectively. The uncertainty due to the trigger efficiency is negligible compared to the other uncertainties. All these uncertainties are added in quadrature giving total systematic uncertainties for all modes in the (5.9–6.8)% range.

4. Upper limits on the branching fractions

Finally, we examine the data in the signal region and observe two candidate events for the $\mu^- \pi^+ K^-$ mode, one candidate event for each of the $\mu^- K^+ \pi^-$, $\mu^+ \pi^- K^-$ and $e^+ \pi^- \pi^-$ modes, and no candidate events for the other modes. These numbers of events are consistent with the expected numbers of background events. Since no statistically significant excess of data over the expected background is observed, we set the following upper limits on the

branching fractions of $\tau \to \ell hh'$ based on the Feldman–Cousins method [23]. The 90% C.L. upper limit on the number of signal events including a systematic uncertainty (s_{90}) is obtained using the POLE program without conditioning [24] based on the number of expected background events, the number of observed events and the systematic uncertainty. The upper limit on the branching fraction ($\mathcal{B}$) is then given by

$$\mathcal{B}(\tau \to \ell hh') < \frac{s_{90}}{2 N_{\tau\tau} \varepsilon}, \qquad (1)$$

where $N_{\tau\tau}$ is the number of $\tau^+ \tau^-$ pairs, and ε is the signal efficiency. The value $N_{\tau\tau} = 616.6 \times 10^6$ is obtained from the integrated luminosity times the cross section for τ-pair production, which is calculated in the updated version of KKMC [25] to be $\sigma_{\tau\tau} = 0.919 \pm 0.003$ nb. Table 3 summarizes information about the

upper limits for all modes. We obtain the following 90% C.L. upper limits on the branching fractions: $\mathcal{B}(\tau \to ehh') < (4.4\text{–}8.8) \times 10^{-8}$ and $\mathcal{B}(\tau \to \mu hh') < (3.3\text{–}16) \times 10^{-8}$. These results improve upon previously published upper limits by factors of 1.6 to 8.8 [10].

5. Summary

We have searched for lepton-flavor and lepton-number-violating τ decays into a lepton and two charged mesons ($h, h' = \pi^{\pm}$ or $K^{\pm}$) using 671 fb^{-1} of data. We found no excess of signal in any of the modes. The resulting 90% C.L. upper limits on the branching fractions, $\mathcal{B}(\tau \to ehh') < (4.4\text{–}8.8) \times 10^{-8}$ and $\mathcal{B}(\tau \to \mu hh') < (3.3\text{–}16) \times 10^{-8}$, improve upon previously published results by factors of 1.6 to 8.8. These more stringent upper limits can be used to constrain the parameter spaces in various models of new physics.

References

[1] A. Ilakovac, Phys. Rev. D 62 (2000) 036010.
[2] D. Black, et al., Phys. Rev. D 66 (2002) 053002.
[3] A. Brignole, A. Rossi, Nucl. Phys. B 701 (2004) 3.
[4] C.-H. Chen, C.-Q. Geng, Phys. Rev. D 74 (2006) 035010.
[5] E. Arganda, M.J. Herrero, J. Portolés, JHEP 0806 (2008) 079.
[6] T. Fukuyama, et al., Eur. Phys. J. C 56 (2008) 125.
[7] M. Raidal, et al., Eur. Phys. J. C 57 (2008) 13.
[8] M.J. Herrero, J. Portolés, A.M. Rodriguez-Sánchez, Phys. Rev. D 80 (2009) 015023.
[9] S. Kurokawa, E. Kikutani, Nucl. Instrum. Methods A 499 (2003) 1, and other papers included in this volume.
[10] Y. Yusa, et al., Belle Collaboration, Phys. Lett. B 640 (2006) 138.
[11] B. Aubert, et al., BaBar Collaboration, Phys. Rev. Lett. 95 (2005) 191801.
[12] A. Abashian, et al., Belle Collaboration, Nucl. Instrum. Methods A 479 (2002) 117.
[13] K. Hanagaki, et al., Nucl. Instrum. Methods A 485 (2002) 490.
[14] A. Abashian, et al., Nucl. Instrum. Methods A 491 (2002) 69.
[15] S. Jadach, et al., Comput. Phys. Commun. 130 (2000) 260.
[16] D.J. Lange, Nucl. Instrum. Methods A 462 (2001) 152.
[17] S. Jadach, et al., Comput. Phys. Commun. 70 (1992) 305.
[18] F.A. Berends, et al., Comput. Phys. Commun. 40 (1986) 285.
[19] C. Amsler, et al., Particle Data Group, Phys. Lett. B 647 (2008) 1.
[20] S. Brandt, et al., Phys. Lett. 12 (1964) 57;
E. Farhi, Phys. Rev. Lett. 39 (1977) 1587.
[21] K. Sumisawa, et al., Belle Collaboration, Phys. Rev. Lett. 95 (2005) 061801.
[22] K. Abe, et al., Belle Collaboration, Phys. Rev. D 66 (2002) 032007.
[23] G.J. Feldman, R.D. Cousins, Phys. Rev. D 57 (1998) 3873.
[24] See http://www3.tsl.uu.se/~conrad/pole.html;
J. Conrad, et al., Phys. Rev. D 67 (2003) 012002.
[25] S. Banerjee, et al., Phys. Rev. D 77 (2008) 054012.